放送大学研究年報　第14号（1996）137－172頁
Journal of the University of the Air, No.14 (1996) pp. 137－172

The structure of water as revealed by spectroscopic methods

Yoshiaki HAMADA* and Kikuko FUKUMOTO**

分光法でみた水の構造

濱田嘉昭*、福本喜久子**

要旨

振動および回転分光法で研究された水の構造に関する現在の理解について概観した。一つの水分子の構造の正確で精密な構造決定でさえも現在的な研究課題である。分子構造は測定データの解析に用いられる理論に依存し、そして何よりもデータの質に依存するのであるが、これらの理論や測定装置は現在も活発に開発されているのである。

液体の水の構造は測定に用いた方法に依存しており、時間的にどの段階の姿を見るかで異なっている。すなわち，液体の水は流体力学的に静止した状態でもpsの時間スケールでの動的な運動を行っており，数１０から数１００Åにわたる空間的に階層化された構造を持っている。水の構造の理解は分子レベルでの生命活動の研究には欠くことのできない要件である。本稿の最後に高分子と水の相互作用に関してＲａｍａｎ分光法で調べた我々の研究の結果を述べた。

The original principle of all things is water,
from which everything proceeds and
into which everything is again resolved.
(Thales, 624?-547? B.C.)

1. Introduction

Water is one of the universally existing materials on the earth, and the characters of its every phase, gas (vapor), liquid, and solid (ice), and the change of the phases are strongly correlated with the natural phenomena and life processes. The reason is that water is not only abundant material but also has unusual chemical and physical characteristics compared to the other related compounds. We need to

* 放送大学助教授（自然の理解専攻）
** 放送大学教務補佐員

know that the existence of all the living things is allowed under very delicate and dynamic balance of the phases of water and its special characters.

The available water is distributed over the surface of the earth in a very uneven manner. The oceans of 3.6 x 10^8 km^2 area contain 13 x 10^8 km^3 of water and occupy 97% of all the quantities of water on the earth. Only 3% is fresh water, but 75% of them are freezed as the Arctic and Antarctic ice caps and remaining 25% are subterranean water. Thus, less than 0.027% of the total water is fresh and immediately available. The distribution of water on the earth is shown in Fig. 1.

Our human body (adult) is constituted of about 65 wt% of water. We excrete 2.5 *l* of water (feces and urine:65%; sweat:20%; expiration:15%), and take 0.3 *l* of water as foods. Therefore we need to drink 2.2 *l* of water a day to keep the balance.

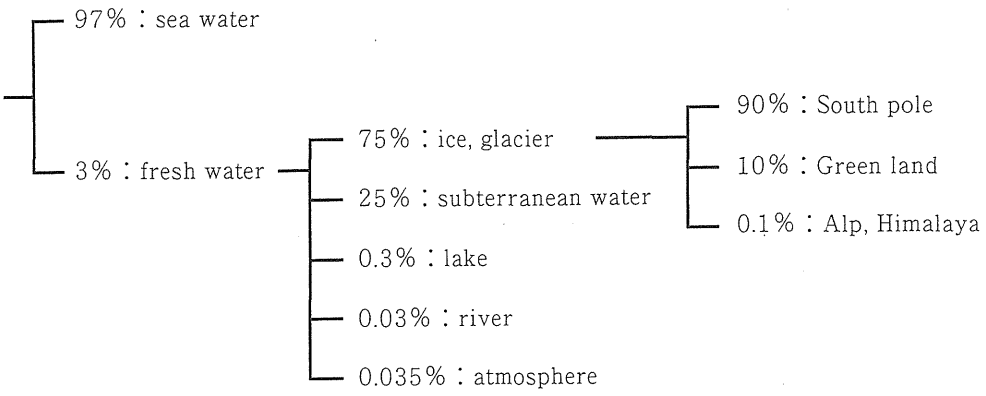

Fig. 1 Water on the Earth (from ref. 3)

Water had been recognized as one of the fundamental materials from the beginning of the civilization of human history, and still now the importance of the studies on water is growing from the standpoint of ecology and life activities. The survey of the studies on water cannot be extensive, since the number of studies will be of the order of thousands a year, or more. Review works and books have been published time to time, reflecting the current understandings on water[1-6].

In this artcle we review the current understandings on the structure of water studied by vibrational and rotational spectroscopy. It should be realized that accurate and precise determination of the structure of free single water molecule is still one of the contemporary researches. It highly depends on the development of the theory appropriate to the analysis of the experimental data. The quality of the data is an index of the performance of the measurement apparatus, which is also rapidly developing now.

The structure of the liquid water is described differently depending on the method used for the measurement, which observe the structure in a different time scale. That is, the liquid water should be understood to have dynamic motions in ps time order and have spatially classified structures in a few 10 to 100 Å order even under hydrodynamically stable condition. The understanding of the water structure is inevitable for the investigation of the life processes at molecular level. At the last section of this article, we present our preliminary results on the interaction of water with polymers studied by Raman spectroscopy.

2. Structure of the free water molecule

Generally the structures of free molecules are determined by the analysis of the pure rotation and/or vibration-rotation spectra. The typical example of the pure rotation spectrum of diatomic molecule is shown in Fig. 2. The rotational energy of diatomic molecules are approximately described by $E(J)=BJ(J+1)$, where J is the rotational quantum number and takes only an integer. The selection rule of the transition is derived from the quantum mechanical consideration to be $\Delta J=\pm 1$. Therefore, the spectral position of the transition $J+1\leftarrow J$ is calculated to be $F(J) = E(J+1)-E(J)=2B(J+1)$. This equation predicts that the spectrum shows an equidistant spacing of $2B$ as is actually observed for the case of CO (Fig.2).

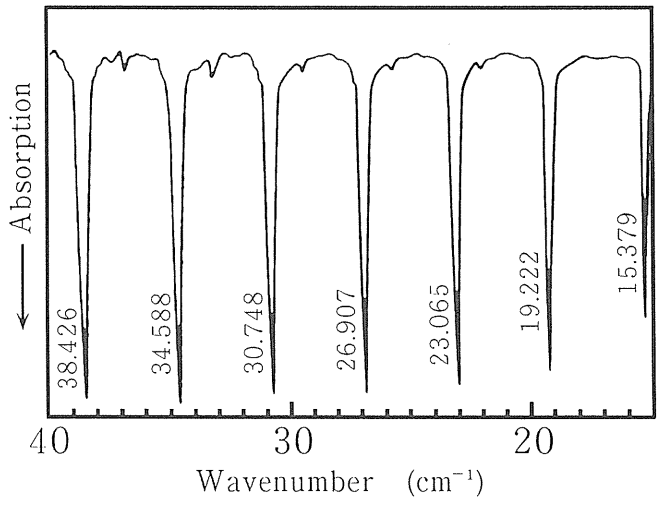

Fig. 2 Far-infrared Pure Rotation Spectrum of CO
(from J.M. Hollas, "High Resolution Spectroscopy" Butterworths, London (1982))

We can thus determine the rotational constant B experimentally. The parameter B is related to the moment of inertia I as follows

$$B=\frac{h}{8\pi^2 I_B} \quad [\mathrm{Hz}] \qquad 1)$$

where I is the function of the atomic weights and positions of atoms in the molecule such that

$$I=\sum_i m_i r_i^2 \quad [\mathrm{amu}\cdot\mathrm{\AA}^2] \qquad 2)$$

Since the atomic weights m_i are already known, the experimentally obtained parameter B gives the information on r_i, that is, the interatomic distance.

The number of structural parameters of H_2O molecule is two under the assumption of C_{2v} symmetry as it is. They are r(O-H) and α ($\angle$H-O-H). Therefore we need at least two independent observables. We can determine experimentally three principal moments of inertia, I_A, I_B, *and* I_C, through the analysis of pure rotation and/or vibration-rotation spectra. The spectrum is not so simple at a glance as that of the diatomic molecule, but can be analyzed as a superposition of subbranch patterns, each of them has some special regularity. If we take the Cartesian coordinates as defined in Fig. 3, the principal moments of inertia are described as follow,

$$I_A=\sum_i m_i y_i^2,\quad I_B=\sum_i m_i x_i^2,\quad I_C=\sum_i m_i(x_i^2+y_i^2) \qquad 3)$$

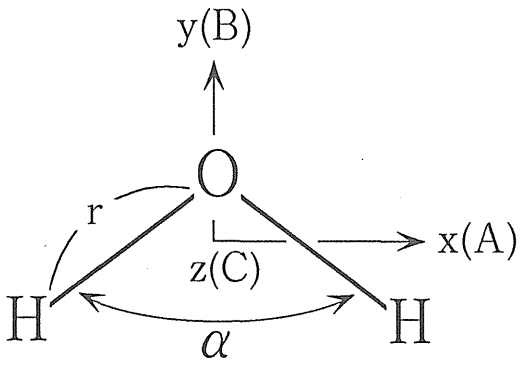

Fig. 3 Structural Parameters of Water

In case of XY_2 type molecule like water, the internal coordinates (r, α) and Cartesian coordinates can be definitely related, and the formula 3) can be rewritten as follow

$$I_A=I_{xx}=\frac{2m_H m_O}{M}r^2\cos^2\frac{\alpha}{2},$$

$$I_B = I_{yy} = 2\, m_H r^2 \sin^2 \frac{\alpha}{2}, \qquad 4)$$

$$I_C = I_{zz} = I_B + I_A$$

where M is the total mass of the molecule. Therefore, the parameters, r, α, are easily evaluated to be

$$r^2 = \frac{1}{m_O} I_A + \frac{1}{2\, m_H} I_C, \quad \tan^2 \frac{\alpha}{2} = \frac{m_O}{M} \frac{I_B}{I_A} \qquad 5)$$

Herzberg[7] listed three independent rotational constants, A_0, B_0, and C_0 determined from the microwave spectrum of the ground vibrational state where suffices 0 stand for v(vibrational quantum number)$=0$. From these constants we can calculate the moments of inertia to be $I_A = 0.6047$, $I_B = 1.162$, and $I_C = 1.816$ amu • Å^2. Using the formula 5), the structural parameters are derived to be

$$r_0 = 0.969 \text{Å}^2 \text{ and } \alpha_0 = 105.1^\circ \qquad 6)$$

If the molecule is planar, all the three moments of inertia are not independent each other, and the inertial defect defined as

$$\Delta = I_C - (I_A + I_B) \qquad 7)$$

should be zero. In fact, Δ of H_2O of the ground vibrational state is close to zero, but not exactly so. The Δ value calculated from the moments of inertia described above is

$$\Delta = 0.049 \text{ amu} \cdot \text{Å}^2 \qquad 8)$$

Therefore, the structure determination from the rotational constants has some ambiguity depending on the combination of the rotational constants chosen. The rotational constant is the physical quantity which reflects the geometrical positions of particles in the molecules, but also it includes the effects of vibrational motion, centrifugal distortion, and electronic excitation. The details of inertial defect was analyzed by Oka and Morino[8].

One of the ways to eliminate the complex effects described above is to obtain the equilibrium rotational constants or equilibrium moments of inertia. The equilibrium constants are extrapolated by using the following equation

$$B_v = B_e - \sum \alpha_i^B \left(v_i + \frac{d_i}{2} \right) \qquad 9)$$

The equilibrium values are believed to be minimized from the contributions of

vibrational, isotopic, and the other effects. The vibration-rotation constants α are the function of rotational constants, harmonic frequencies, anharmonic constants, and Coriolis interaction constants. Its formula were derived by Darling and Dennison[9,10] by the second order perturbation theory. Using the rotational constants of the ground vibrational state[10] and α values determined by Benedict et al.[12], the equilibrium values were estimated[13] to be

$$r_e = 0.9575\text{Å} \text{ and } \alpha_e = 104.51^\circ \qquad 10)$$

Great efforts have been paid to obtain the accurate potential energy functions which reproduce the observed vibrational and rotational energy levels. Hoy and Bunker[14] applied non-rigid bender model[15,16] to the experimental energy levels obtained by infrared (IR) and microwave spectroscopy until that time and deduced the values,

$$r_e = 0.95781(3)\text{Å} \text{ and } \alpha_e = 104.4776(19)^\circ \qquad 11)$$

Jensen[17] combined Morse oscillator and rigid-bender model and fitted to the experimental energy levels with the bending parameter constrained to the best ab initio value[18] at that time, and gave the structural parameters to be

$$r_e = 0.95843(1)\text{Å} \text{ and } \alpha_e = 104.43976^\circ \qquad 12)$$

Recently Jensen combined the non-rigid description of the bending and rotation motions with a Morse oscillator description of the stretching motion[19]. He optimized the parameters of this Hamiltonian, MORBID (Morse Oscillator-Rigid Bender Internal Dynamics), to 2383 vibration-rotation energy spacings involving the rotational quantum numbers $J \leqq 10$ in 120 vibrational states extending up to 19000 cm^{-1} above the vibrational ground state for 10 isotopomers[20]. The root-mean-square deviation of the fitting was 0.36 cm^{-1} and 28 parameters were determined. The equilibrium bond length and bond angle were estimated to be

$$r_e = 0.957848(16)\text{Å} \text{ and } \alpha_e = 104.5424(46)^\circ \qquad 13)$$

respectively. He stated that these are the most accurate equilibrium values currently available for the water molecule. There are some other theoretical studies which reproduce highly excited rotational states or highly excited vibrational states[21,22].

3. Structures of Water Oligomers

3-1. Dimer

The water dimer has attracted much attention of spectroscopists for many years as a starting point for understanding the structure and dynamic behavior of the liquid water.

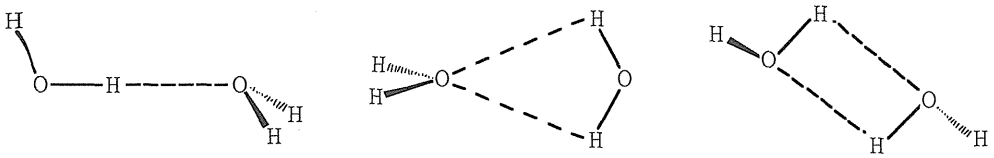

Fig. 4 Possible Structures of Water Dimer

One of the earliest spectroscopic studies on the water dimer had been carried out by van Theil et al.[23]. They observed the IR spectrum of water isolated in solid nitrogen at 20 K. They proposed a cyclic conformation with two bent hydrogen bonds, since they identified only three bands in the region of the perturbed monomer fundamentals. On the other hand, Tursi and Nixon proposed an open non-centrosymmetric structure since they found six bands of the dimer[24]. The theoretical studies also supported the open structure[25,26]. Detailed vibrational assignments of the matrix isolated water have been continued until the present time[27,28] and the rotational motions of water in low temperature matrix have also been an important and interesting subject[29,30].

The first gas phase detection of the water aggregates was done by Greene and Milne[31]. The symmetric structure was excluded from a large dipole moment of the dimer observed by an electric deflection experiment[32]. The bifurcated structure of the most stable dimer has been confirmed through the molecular beam electric resonance spectroscopy by Dyke et al.[33,34]. They observed radiofrequency and microwave transitions of the dimers including D and ^{18}O isotopes. The relative orientation of the two monomer units has been determined by the electric dipole moment component along the *A* inertial axis. The structure of "trans-linear" complex thus obtained is shown in Fig. 5.

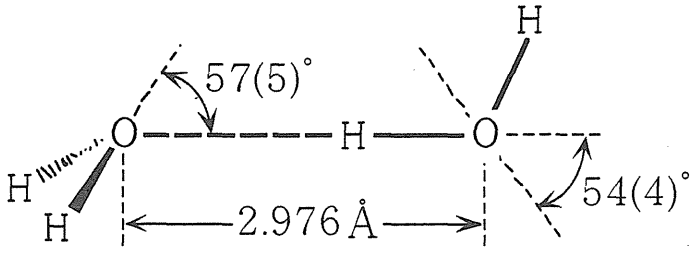

Fig. 5 Structure of Water Dimer (from ref. 34)

Since then, the gas phase spectrum of the ground vibrational state originated from a large amplitude tunneling motion has been the subject for microwave to submillimeter spectroscopy[35,36] Hougen applied his framework theory to the complicated rotational spectrum of the water dimer[37-39]. There exist eight isoenergetic minima which are accessible at the zero point level of excitation. The tunneling motions among these minima give rise to extremely complicated energy levels. One of the tunneling motions is that the two H_2O subunits interchange proton-donor and proton-acceptor bonding role in the complex. The other is the twofold rotations of either or both of the water units about their C_2 symmetry axes (see Fig. 6). The observed ground state spectrum until 1991 and its group theoretical treatment were summarized by Fraser[40].

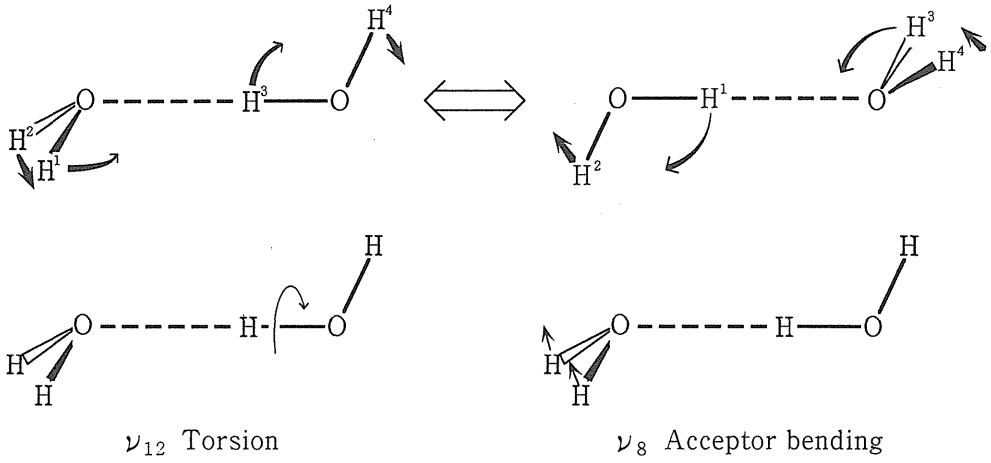

Fig. 6 Tunneling Motions of Water Dimer

Geared tunneling motion (upper) interchanges the donor-acceptor role in the dimer. The two lowest frequency normal modes (lower) affect the interconversion tunneling splitting.

The accurate measurement of the intermolecular vibration of the water dimer has been done successfully by Saykally et al.[41]. They observed five vibration-rotation-tunneling bands of $(D_2O)_2$ near 84 cm^{-1}. The spectrum indicates a strong coupling of both the donor-acceptor interconversion and donor tunneling motions.

The dynamic behavior of the water clusters was studied by detecting the recoiling fragments off-axis from the molecular beam as a function of laser frequency using a rotational mass spectrometer[42]. The clusters formed in the molecular beam are predissociated by tunable, pulsed, infrared radiation in the frequency range 2700-3750 cm^{-1}. It was found that the spectra of clusters containing three or more water molecules absorb the same frequency as that of the liquid. An upper limit to the excited vibrational state lifetime is about 1 μs.

3-2. Trimer

Little information has been available for the trimer and higher oligomers of water compared to the dimer. Theoretical calculations suggested a stable cyclic conformation of the trimer[43].

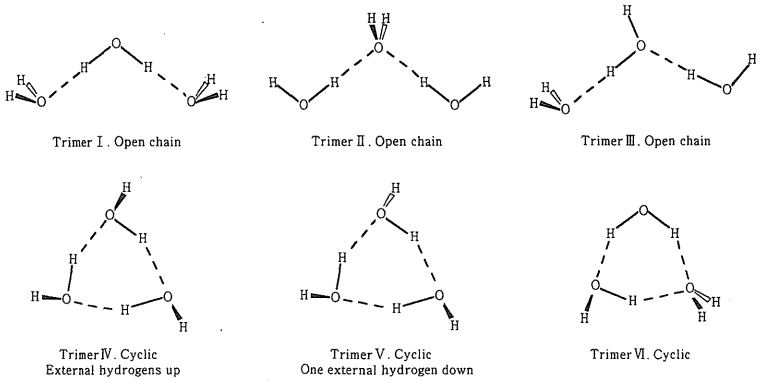

Fig. 7 Possible Structures of Water Trimer

Dyke and Muenter suggested a cyclic structure of the water trimer, because of a small dipole moment obtained from their molecular beam deflection experiment[32]. Kistenmacher et al. reanalyzed a large number of Hartree-Fock computations for the water-water interaction and studied small clusters of the water molecules[44]. They supported the cyclic structure for the trimer. On the other hand, Bentwood et al. concluded an open-chain structure for the water trimer isolated in a low temperature argon matrix[45]. The reason was that the IR bands at 3612 and 1602 cm^{-1} attributed to the trimer are expected for the proton acceptor water molecule, whereas the cyclic trimer contains only the donor/acceptor molecules. Nevertheless, their conclusion remained uncertain.

Engdahl and Nelander extended the IR spectral data of all H- and D- containing trimers in argon and krypton matrices[46]. A detailed identification of the bands and the normal coordinate analysis showed that the peak positions and intensity predictions calculated for the cyclic model agree with the observed spectra. Therefore, they concluded the cyclic structure with its three water molecules all equivalent.

Saykally et al. constructed an experimental system to observe the high resolution far-infrared spectrum (with tunable FIR lasers) of low-frequency van der Waals vibrations in weakly bounded clusters (produced by supersonic expansion)[47, 48]. The spectrum of $(H_2O)_3$ observed showed a strongly perturbed near-symmetric-top rotational pattern with each rovibrational transition split into four components as shown in Fig. 8[49].

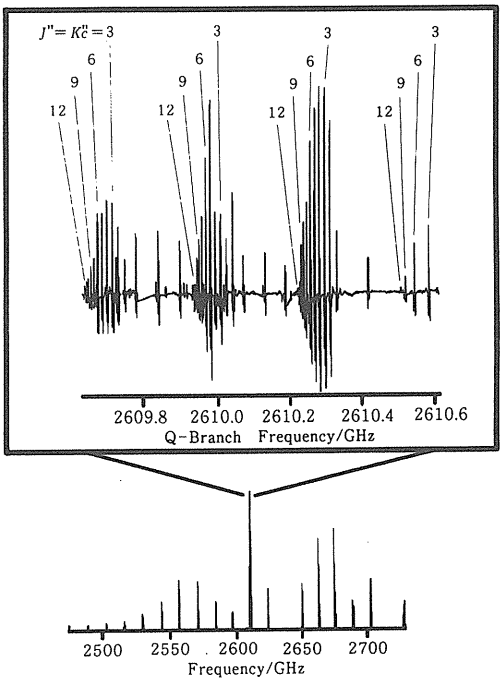

Fig. 8 Far-Infrared Spectrum of Water Trimer (from ref. 49)

In one of the four bunches of transitions (upper trace), spectral lines of $K_c \neq 3n$ are missing because of their vanishing spin statistic weight. This confirms the symmetry group G_{48} of the water trimer.

The spectral splittings were interpreted as resulting from the isomerization tunneling motions among 96 identical frameworks (or 48 pairs of enantiomers) via three low energy barrier pathways. Two of them are shown in Fig. 9. At the equilibrium geometry, two of the free hydrogens lie above the ring and one below. The second pathway in Fig. 9, 'donor tunneling pathway', is a possible mechanism that exchanges the hydrogen-bonded and free hydrogens on one water monomer, any of which could give rise to the observed quartet splitting in the spectra. The third pathway is a concerted motion that reverses the sense ('clockwise' or 'counterclockwise') of the hydrogen-bonding network around the ring.

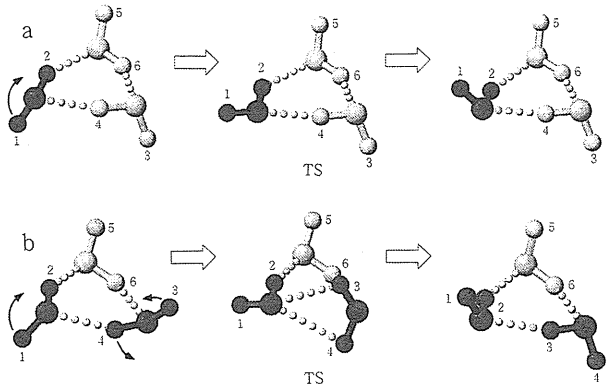

Fig. 9 Tunneling Motions of Water Trimer (from ref. 49)

Three water molecules are connected by hydrogen bond and make a ring in which each molecule acts as a proton donor and acceptor. Two of the free hydrogen atoms lie above the ring and one below. a) shows 'flipping pathway' where one water molecule (shaded) rotate about its donated hydrogen bond. TS is a transition state where two free hydrogen atoms are on opposite sides of the ring and one is in the plane. Through this motion, a given global minimum structure (left/right) transform to its enantiomeric structure (right/left). b) shows 'donor tunneling pathway' where two water units (shaded) having their free hydrogen atoms on opposite sides of the ring are involved in the tunneling motion. The free hydrogen atom of the 'donor' molecule moves into the ring and at the same time the bonded hydrogen of the molecule is pushed away on the other side of the ring. In consequence, the two free hydrogen atoms of the two units are exchanged through the bifurcated transition state where the free hydrogen atom of the 'acceptor' molecule lie on the ring plane.

Their work stimulated a number of theoretical calculations of the structure, vibrational frequencies, and interconversion tunneling dynamics[50-54]. The experimental and high level theoretical studies are still in progress. From these studies we will be able to elucidate the details on cluster structure, intermolecular potential, and tunneling dynamics of water.

4. Structure of Ice

It is known that there are more than 10 phases for ice, that is, ice shows a polymorphism. The phase of ice which arises under the ordinary condition (near the triple point) is called ice I. The phase diagram of water is shown in Fig. 10.

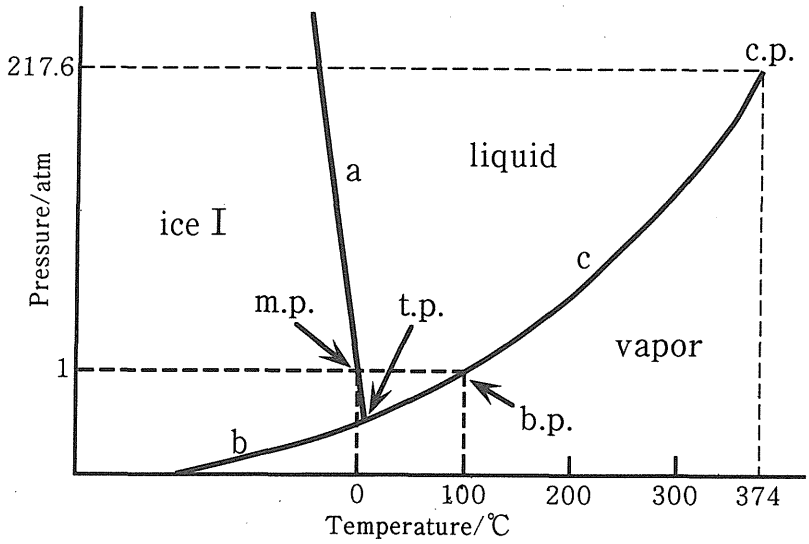

Fig. 10 Phase Diagram of Water

a: melting curve, b: sublimation curve, c: evaporation curve,
m.p.: melting point (273.15 K), b.p.: boiling point (373.15 K),
t.p.: triple point (273.16 K), c.p.: critical point (647.30 K)

The equilibrium line between solid and liquid, that is the melting curve, has a negative slope or goes down towards right. The relation between pressure and temperature at the boundary of two phases is given by Clausius-Clapeyron equation as

$$\frac{dP}{dT} = \frac{\Delta H}{T\Delta V} = \frac{\Delta S}{\Delta V} \qquad 14)$$

where ΔH, ΔS, and ΔV are phase transition enthalpy difference, phase transition entropy difference, and volume change caused by the phase transition. The negative slope $dP/dT<0$ of the melting curve means $\Delta V<0$ since the transition from ice to liquid water is endothermic, that is $\Delta H>0$. The volume of water decreases when it changes from ice to liquid as is observed in the natural phenomenon. It then turns out that the melting entropy is positive $\Delta S>0$. In general, the degree of freedom of motion decreases when the volume of material decreases, this means the entropy should decrease. This anomaly of water will be discussed later. Anyway, the negative slope of the melting curve reflects the fact that ice melts to the liquid water when ice is given a pressure near the equilibrium temperature. That is the reason why we can skate on ice, eliminating the friction between ice and shoe edge by the interfacial water.

The structure of ice was determined by X-ray diffraction first. The exact position of hydrogen atoms was provided by the neutron diffraction method[55,56]. The structural parameters thus determined are shown in Fig. 11.

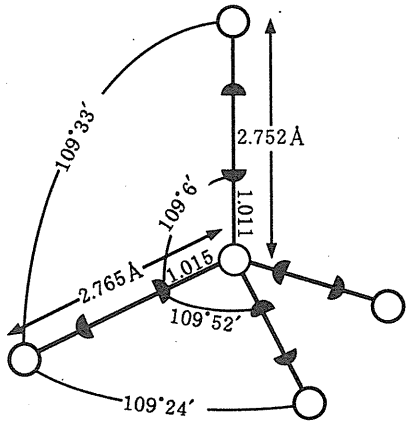

Fig. 11 Structure Determined by Neutron Diffraction

To explain the diffraction data, half a hydrogen atom had to be supposed to locate at 1.015 Å from O atom. This means that the hydrogen atoms are not fixed spatially in ice, but go and back among the two equilibrium positions between O⋯O. That is, ice is constituted by a network of O atoms connected by the hydrogen bonding. This fact, that the positions of hydrogens are not fixed in the solid state but there is a disorder in space configuration, is shown thermodynamically as a residual entropy of ice.

According to the third law of thermodynamics, the entropy of crystalline material at 0 K should be zero, and in fact there are many experimental evidences to support the law. But in case of ice, there does exist $S_0 = 3.4\ \mathrm{J\ K^{-1}\ mol^{-1}}$ [57]. The thermodynamical entropy S as a macroscopic physical quantity is related with W as a number of microscopic states by

$$S = k \ln W \qquad 15)$$

where k is Boltzmann constant.

Pauling[58] proposed the following assumptions for ice,

1) Hydrogen atoms in ice locate on O⋯O axis, and there is two stable positions on each O⋯O line.

2) The water molecule in ice exists as neutral H_2O.

and made a consideration with statistical thermodynamics. Total number of configurations of hydrogen atoms in 1 mol ice is $W' = 2^{2N_A}$. There are 4 nearest O atoms for each oxygen atom. Therefore, totally 16 cases are possible for the configurations

of hydrogen atoms around each O atom as shown in Fig.12.

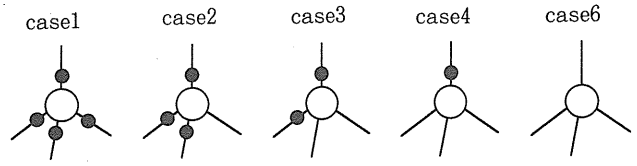

Fig. 12 Possible Configurations of Hydrogen Atoms in Ice

Among these possible configurations, only the case 3 meets the second condition described above. Therefore, weight factor 6/16 should be applied to count the number of configurations for each O atom. Finally, the entropy of ice at 0 K is calculated to be

$$S=k\ \ln W=k\ \ln\left(\frac{6}{16}\right)^{N_A}\cdot 2^{2N_A} \quad =k\ \ln\left(\frac{6}{16}\cdot 2^{2}\right)^{N_A}$$

$$=k\ N_A\ln\left(\frac{3}{2}\right)=3.37\text{J K}^{-1}\text{mol}^{-1}$$

This explains the experimental value described above.

There are two forms for ice I, that is ice I_h and ice I_c. The ice I_c is obtained when the vapor is directly solidified under -120℃. Ice I_c changes into ice I_h when it is heated above -100℃. Therefore ice I_c is a metastable phase.

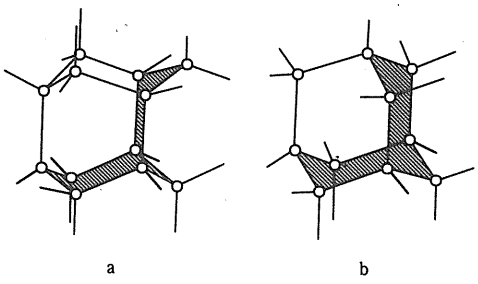

Fig. 13 Two Structures of Ice I

a: ice I_h, b: ice I_c

The structures of ice I_h and I_c are shown in Fig. 13. There are 4 nearest O atoms for each O atom. In each crystal form, chair forms made of 6 O atoms are connected

transversely via hydrogen bonding, and make two dimensional network. These networks are piled up and make three dimensional network via hydrogen bonding. Again sexangle configurations are formed longitudinally. But the difference occurs here for ice Ih and Ic, the former makes a boat form and the latter makes a chair form. The bond distances between the nearest O atoms are 2.74 and 2.75 Å for ice I_h and I_C, respectively. Both of the crystal forms have fairly large opening spaces, and the densities are 0.94 (at -175℃, 1 atm) and 0.93 g cm^{-3} (at -130℃, 1 atm) for ice I_h and I_C, respectively.

I'm facing river Nemunas
Surrounded by forest and green grass
Its surface reflecting sky above
My face it mirrors deep below
Wonderful world!
Wonderful water!
How can Nature make
Such beautiful liquid thing
Hydrogen bond, of course!
Link it together
Through hexagonal rings.
(Prof. G. Aksncs, at XIth Int. Workshop
"Horizons in Hydrogen Bond Research"
Vilnius Univ. Lithuania 1995)

5. Liquid Water

5-1. Special Characters of Water

Temperature on the earth surface does not change more than a few ten degree in spite of the large change of heat supply from the sun depending on day and night, summer and winter. The change of body heat should be kept within a few degree. These homeostasis are realized by the special thermochemical characters of water. Typical thermochemical characters are shown in Fig. 14 to 16, and compared with those of the related compounds, the hydrides of the elements of the same row and group in the periodic table.

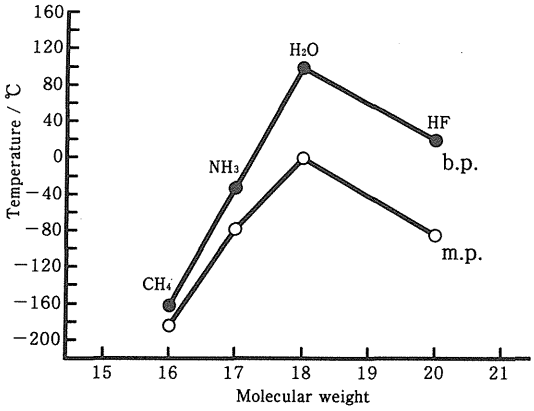

Fig. 14 Boiling(●) and Melting(○) Points of the Second Row Hydrides

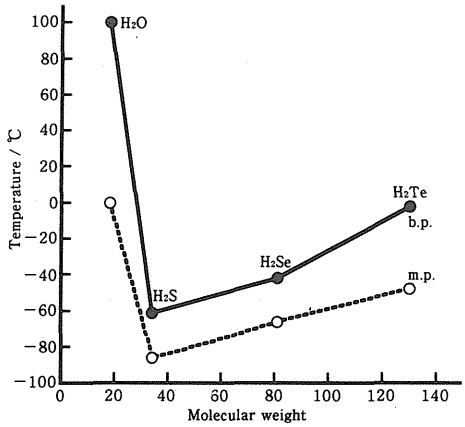

Fig. 15 Boiling(●) and Melting(○) Points of the Group 6B Hydrides

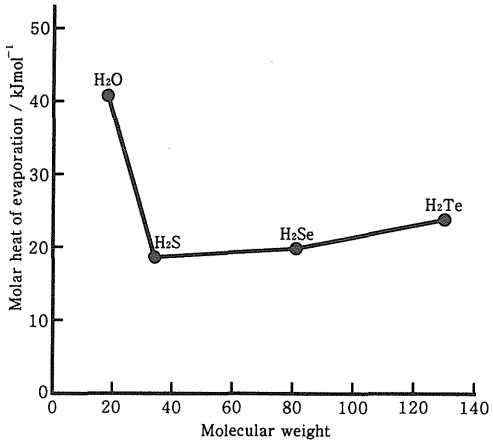

Fig. 16 Molar Heat of Evaporation of the Group 6B Hydrides

If the characters of water could be interpolated from the related molecules against the molecular weight, water would freeze at about −91℃ and boil at about −73℃. Temperature of water would go and down 2 or 3 times faster than the real water against the temperature changes of the environments.

The densities of most of the materials increase when the phase changes from liquid to solid by the temperature decrease. Therefore, the solid material sinks down in the system where the liquid and solid coexist. In this point, water behaves differently. The densities of water near 0℃ are shown in Fig. 17.

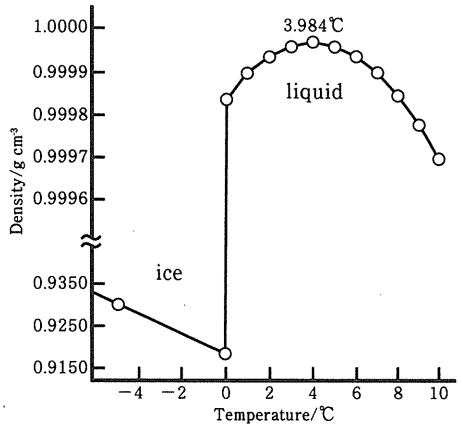

Fig. 17 Densities of the Water near 0℃
Maximum density (1.000 g/cm^{-3}) is at 3.984 ℃.

Generally the densities of liquid decrease with increasing temperature, that is the average intermolecular distance increases because of more active motions of molecules at higher temperature. Nevertheless, the density of water increase starting from 0℃, reaches maximum at 3.98℃, and then decreases.

This unusual character compared to the other solvent makes it possible that ice can float on water. Otherwise, water of lake and river starts to freeze from the bottom and water above is brought directly contact with cold environment, and consequently the lives in water cannot be secured.

5-2. Structure of Liquid Water

One of the characteristics of fluid is that the volume is constant but the shape is variable and can be stored in any form of the bottle. Doesn't water have any kind structure? It is difficult to recognize at a glance that the ice of glacier is streaming always. But the position of a rock on the glacier or the shape of the glacier itself are not those of one year ago. The change of the shape or structure of the glacier

depends on the time scale you observe it. The same consideration can be applied to the structure of water.

Eisenberg and Kauzmann classified the structures of water depending on the time scale of observation.

(a) I-structure: the instantaneous structure observed within the time scale faster than the molecular vibrations ($t < \tau_V$).

(b) V-structure: vibrationally averaged structure, but observed faster than the diffusional motions ($\tau_V < t < \tau_D$).

(c) D-structure: diffusionally averaged structure($\tau_D < t$).

The time scales of the vibrations and diffusion motions in the liquid water are about 10^{-16} and 10^{-10} s, respectively. Therefore the structure determined depends on the experimental method as shown in Fig. 18.

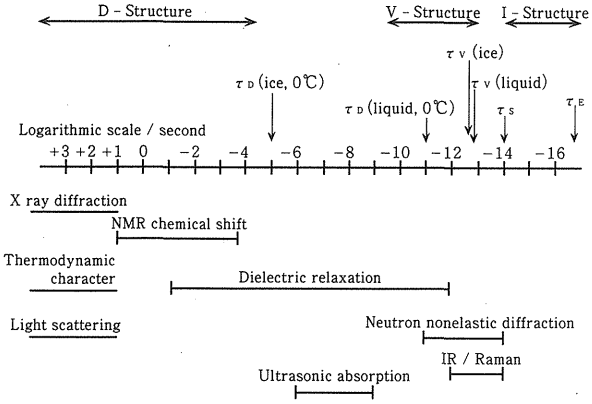

Fig. 18 Relation of the Structures and Experimental Methods

τ_V: vibration frequency, τ_D: diffusion period, τ_E: time for an electron to move around Bohr orbital.

The results of computer simulations corresponding to the three structures described above are shown in Fig. 19 to 21.

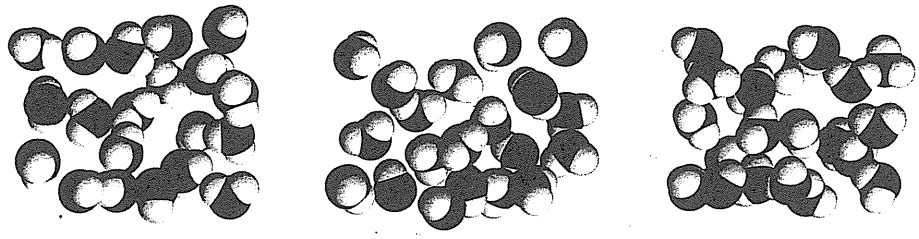

Fig. 19 I-Structure of Water

Some of the typical aggregations of water molecules, each molecule has a different bond lengths and angle deviated within a mean amplitude of vibrations.

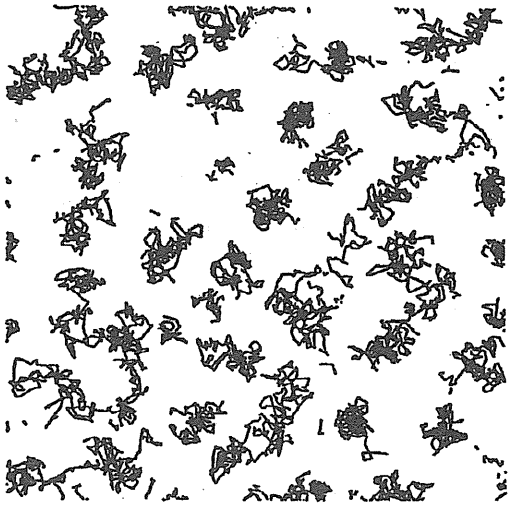

Fig. 20 V-Structure of Water

Traces of the centers of mass of the water molecules in 10 ps. MD calculation by Dr. Hideki Tanaka (from ref. 6).

The D-structure of the liquid water was studied by Morgan and Warren[59] by using X-ray diffraction, and Narten et al.[60] refined the study. One of the results from the observed radial distribution function is that the number of the nearest neighbor oxygen atoms is 4.4 which locate about 2.9 Å from the central oxygen atom. These fundamental atoms seem to exist as the tetrahedral structure like ice I_h.

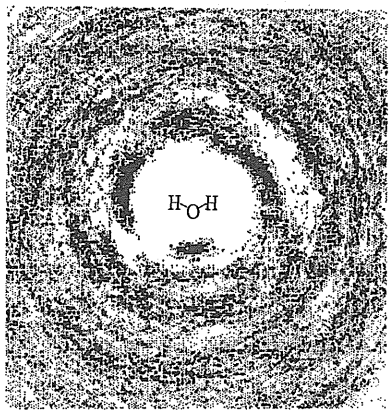

Fig. 21 D-Structure of Water

Distribution of the water molecules observed from the center of mass of the particular water molecule. Monte Calro calculation by Dr. Susumu Okazaki (from ref. 6).

There are broad distribution from 3.5 to 5.5Å, and these atoms make a disorder structure.

Several models were proposed to explain the observed radial distribution function. Nemethy and Scheraga[61] proposed a mixture model where there is an equilibrium between the species which make a cluster by hydrogen bonding between the nearest neighbor molecules, and the monomer species without hydrogen bonding. Morgan and Warren[59,62] proposed a interstitial model where the monomer molecules are inserted into the open space in the framework of hydrogen bonded system. Pople[63] proposed a distorted hydrogen-bond model where every water molecule is hydrogen-bonded with 4 nearest neighbor molecules with a constant O···O distance. The hydrogen bondings are not broken as is supposed in the two models described above, but are distorted at melting.

Recently, Rice and coworkers presented a random network model based on the experimental informations on the structure and dynamics of the molecular motion[64]. The basic assumptions of the model are 1) there is a continuous, albeit distorted, network of hydrogen bonds in the liquid, and 2) it is meaningful to describe the molecular motion by using two distinct time scales. The model could describe the observed r (O − O) distribution function, the dielectric constant, and the bulk thermodynamic properties of the liquid water.

5-3. Molecular Dynamics Simulation on the Liquid Water

Molecular dynamics (MD) calculation is a very powerful technique to investigate the time evolution of the bulky molecular system, and had instantly been applied to the liquid water[65] at the earliest stage of the application. Since then, many new ideas and techniques have been incorporated in the MD simulation[66-68].

Old models on the liquid water have been critically examined and a new concept of the dynamic structure is now showing up. According to the recent MD simulations by Ohmine et al.[69-71], the view of the microscopic structure of liquid water can be described as follow.

In liquid, 10-50 molecules are localized in space and construct an inherent structure in 10 ps time order. Within this time period, the molecules in a group make collective motions, the energy fluctuation caused by each structure change is 10-20 kcal/mol. The lifetime of each hydrogen bonding is about 1 to 2 ps, which is about 10 times longer than the libration and rotation motions. In the course of these collective motions within each group, they find a route to exchange some of the molecules among the neighboring groups with a flip-flop mechanism. The energy fluctuation associated with this large structure change is about 1 to 2 kcal/mol, which is smaller than that associated with structure change within the inherent group described above.

6. Vibration Spectrum of Water

6-1. Vibration Spectrum of the Monomer

The free water molecule has three normal modes of intramolecular vibrations. These are, in frequency order, antisymmetric stretching(ν_3), symmetric stretching (ν_1), and bending(ν_2) vibrations as are shown in Fig 22. The observed vibrational frequencies are the differences of the vibrational energy levels which have the anharmonic effects, and are called the fundamental frequencies.

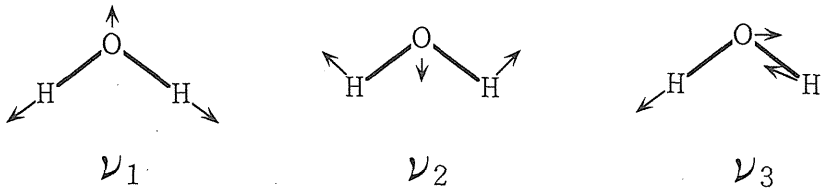

Fig. 22 Three Normal Modes of Vibrations of the Water Molecule

The infrared absorption spectrum of the water vapor is shown in Fig. 23. The spectrum is so complicated because the vibrational transition of the free molecule accompanies the rotational transitions as well. The determination of the fundamental frequencies (rotationless vibration frequencies, or approximately band centers) depends not only on the qualities of the observation (accuracy and the range of assignments of the rotational transitions) but also on the model Hamiltonian used. The best values of the fundamental frequencies[72,73] at the present time are

$$\begin{aligned} \nu_1 &= 3657.0542 \\ \nu_2 &= 1594.7475 \\ \nu_3 &= 3755.9242 \ (\mathrm{cm}^{-1}) \end{aligned} \qquad 17)$$

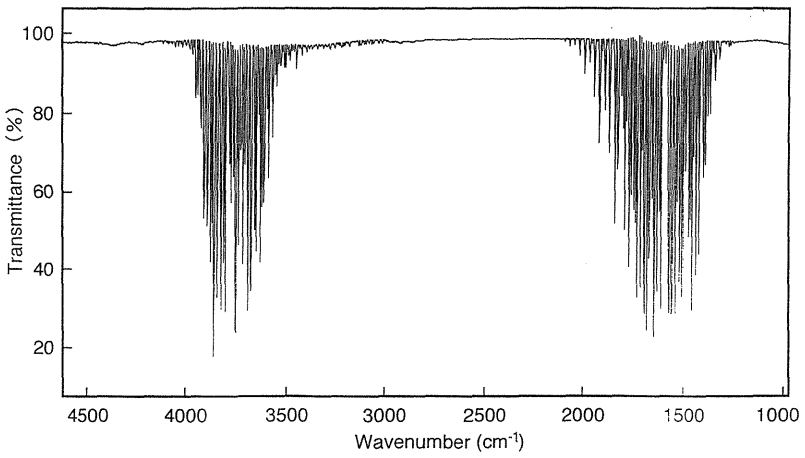

Fig. 23 Infrared Absorption Spectrum of Water Vapor

Spectrum was measured by Bomem FTIR spectrometer under the following condition: vapor pressure ca. 5 torr in 15 cm cell, spectral resolution 0.5 cm^{-1}.

The bending motion has a fairly large amplitude, and displays an anomalous centrifugal distortion. Therefore a finite Taylor series expansion of the angular momentum operators by the Watson-type Hamiltonian is not appropriate for representing high J and K rotational energy levels. A special treatment on the ν_2 band has been reported recently[74]. The potential functions and theoretical representation of highly excited vibrational states of the free molecule are continuing interest[75-77].

The low-temperature rare-gas matrix isolation technique has been widely used to observe the vibration spectrum of the molecule which is free from the complicated rotational transitions. Water has been one of the target molecule since the early days of this technique, and it has been known that the water molecule can rotate even in the solid rare gas matrix. In the most recent paper, Jacox et al. refined the assignments of the spectra of water and its dimer including the isotopomers in solid neon[30]. According to their assignments, the strong absorptions of the water monomer are all include the rotational transitions, for example the strongest transition in each band are

$$\begin{aligned} \nu_1 &: (1_{1,1}\text{-}0_{0,0}) = 3696.9(\mathrm{m}) \\ \nu_2 &: (1_{1,1}\text{-}0_{0,0}) = 1630.6(\mathrm{vs}) \\ \nu_3 &: (1_{0,1}\text{-}0_{0,0}) = 3783.3(\mathrm{vs}) \quad (\mathrm{cm}^{-1}) \end{aligned} \qquad 18)$$

where the symbols in the first and second parentheses of each row are the rotational transition and intensity (m:medium; vs:very strong), respectively. The so-called 0-0 transitions are very weak or practically not observed.

6-2. Vibration Spectra of Ice and Liquid Water

The vibrational spectroscopy is a useful method to study the V-structure of the liquid water. The random network model could reproduce the observed IR and Raman[78,79] spectra of polycrystalline ice I_h and amorphous solid water[80] (Fig. 24). Theoretical studies[81-85] have confirmed that the low-frequency part (around 3200 cm^{-1}) of O-H stretching Raman band has a contribution from the in-phase collective motion[86]. The band appears as the result of the large net polarizability change of the stretching mode. The shape of the band is most strongly influenced by the intermolecular coupling of OH oscillators because of the tetrahedral nature of the hydrogen bonding.

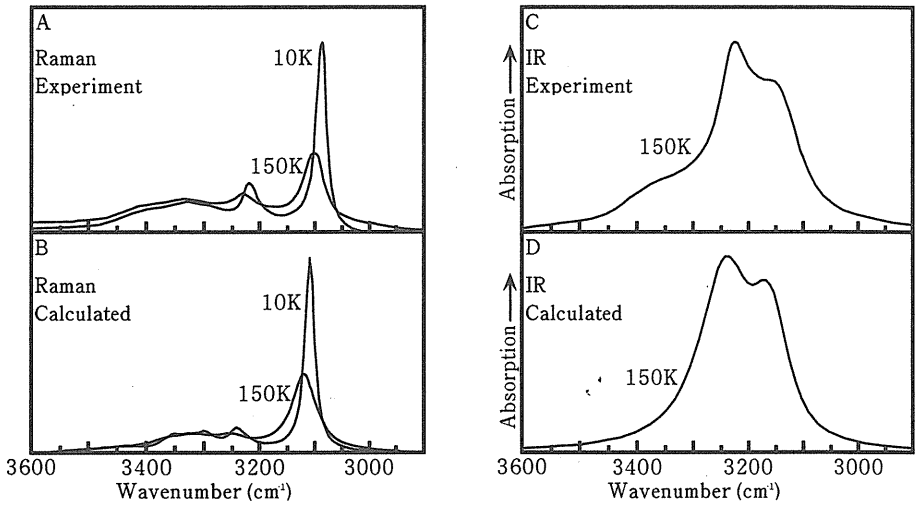

Fig. 24 Comparison of the Observed and Calculated O-H Stretching Band of Polycrystalline Ice I_h

A,B: Raman spectrum; C,D: IR spectrum

Green and co-workers[87] presented a method to deal with the separation of Raman intensity by using a polarization effect, from which we can probe the in-phase collective motion in the liquid water, and the character of the patched structure of the water molecules.

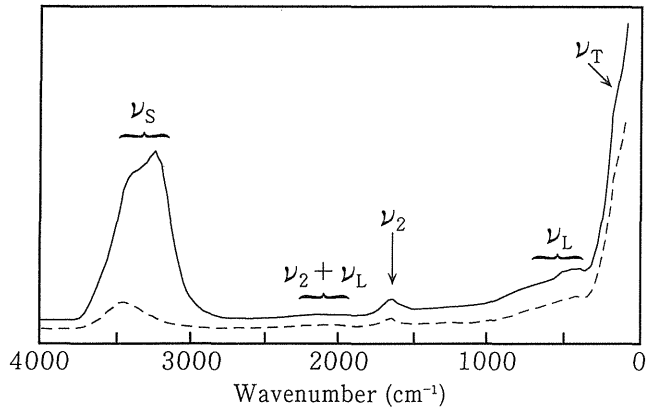

Fig. 25 Polarization Effect of Raman Spectrum of the Pure H_2O Liquid

Parallel (—) and perpendicular (···) spectra at 25℃.
ν_S: O-H stretching modes, ν_2: bending mode,
ν_T: restricted translation modes, ν_L: restricted rotation (libration) modes

Comparisons of the O-H stretching Raman bands of polycrystalline ice, amorphous ice, supercooled melt, and melt of water have lead to the conclusion that the O-H band of water is made of two parts, the lower frequency part reflects the in-phase O-H stretching which is characteristic of ice, and the higher frequency part which is characteristic of amorphous solid water.

The former band is highly polarized, and in practice there is no perpendicular intensity. That is, the perpendicular intensity can be attributable totally to the water of amorphous structure. According to the above discussion, the apparent intensity of parallel component $I_{/\!/}$ can be divided into two components,

$$I_{/\!/}(\omega) = I_{/\!/}^{am}(\omega) + I_c(\omega) \qquad 19)$$

where $I_{/\!/}^{am}(\omega)$ and $I_c(\omega)$ are the intensities originating from the amorphous and structured (or collective) bands, respectively.

The depolarization ratio of the O-H stretching band of the amorphous water is defined by

$$\rho(\omega) = I_{\perp}^{am}(\omega) / I_{/\!/}^{am}(\omega) \qquad 20)$$

Replacing $I_{/\!/}^{am}(\omega)$ of this equation by that of 19), we obtain

$$I_c(\omega) = I_{/\!/}(\omega) - a(\omega) I_{\perp}^{am}(\omega) \qquad 21)$$

where $a(\omega) = [\rho(\omega)]^{-1}$. The spectral curve $I_{\perp}(\omega)$ thus obtained is called the collective band. The intensity of $I_{\perp}(\omega)$ of low frequency side is small, therefore the value of $\rho(\omega)$ is not sensitive to the result. The relative strength of the in-phase collective band is defined by

$$C = \frac{\int I_c(\omega)\mathrm{d}\omega}{\int I_{//}(\omega)\mathrm{d}\omega} \qquad 22)$$

The effects of various types of solutes on C values were studied by Green et al.[88-92]. The integrated intensity of the collective band of the pure water against temperature is shown in Fig. 26. The effect of the hydrogen bond breaking between coupled O-H oscillators caused by translational and/or rotational rearrangement of the water molecules is clearly seen in Fig. 26.

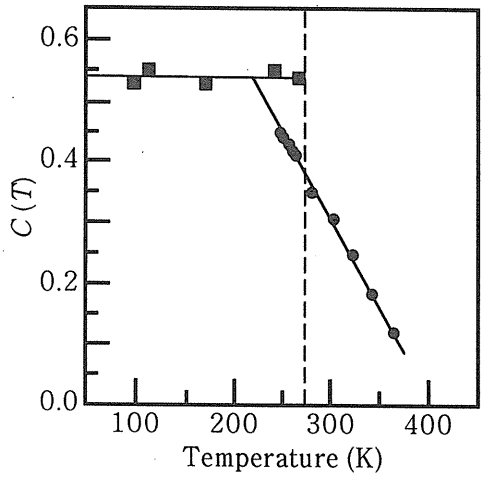

Fig. 26 Variation of the Collective Band of Water against Temperature
■: ice; ●: liquid

The analysis of the collective band in Raman spectrum of water in polymer gels and in aqueous polymer solutions has been carried out[93,94]. The method was useful to clarify the relationship between the size of water domains included in the polymer network and the profile of the O-H stretching Raman band.

Raman and infrared spectroscopic studies on the liquid water until 1970 were summarized by Walrafen[95], and current Raman spectroscopic studies on water in polymer systems were reviewed by Maeda and Kitano[96]

7. Interaction of Water with Protein and Polymer

7-1. Structure of Water Molecules around Polymers

Three phases model for the hydration of proteins has been proposed by Cooke and Kuntz[97], and Uedaira[98]. The concept of the model is shown in Fig. 27.

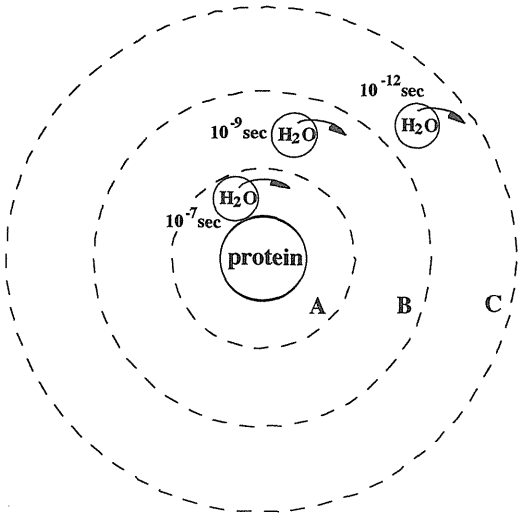

Fig. 27 Hydration Model for Protein in Aqueous Solution

The water molecules bonded directly to the polar groups on the surface of proteins form a monolayer, and is called A phase. These water molecules have rotational relaxation time in the range of $10^{-8}-10^{-7}$ s, and do not freeze down to -190 ℃. The water molecues cannot form a tetrahedral arrangement, because they are strongly attracted to the protein molecule. It is considered that the water molecules of this phase play an important role in the occurrence of protein functions. Also, the water molecules within a protein hydrophobic cavity are inevitable for the protein to give its functions into full play[99].

The water molecules outside the A phase construct the B phase, which has a thickness of a few molecules. Thermal motions of the water molecules in this phase are, more or less, prohibited, since they are affected by the oriented water molecules in the A phase. The rotational relaxation time of these molecules are about 10^{-10} to 10^{-9} s, and do not freeze to about -25℃. This phase has a close correlation with a stability of the protein in aqueous solution.

All the water molecules outside of the B phase form the C phase, that is the ordinary bulk water. The rotational relaxation time is an order of 10^{-12} s.

It is well known that the water molecules around hydrophobic polymers make a specific cluster structure, depending on the character of the polymers. On the other hand, the water molecules around hydrophilic polymers adhere strongly to the surface of the polymer through an electrostatic force. Therefore, they cannot form an oriented structure.

7-2. Denaturation of Protein and Water Structure in Aqueous Solution

Recently, many polymeric materials have been applied in the biomedical and biological fields, such as artificial organs, clinical support devices, drug administration systems, and support matrix to immobilize the enzyme or cell. In applying the polymeric materials to these fields, it is important to consider the interactions between polymers and biological components such as proteins and cells, because the polymeric materials induce biological response. The water molecules are considered to exert a considerable influence on the interaction between the polymers and biological components. Therefore, the information on the water structure in biological system is important in understanding the life processes in molecular level.

Water molecules in contact with a protein have a specific structure, and those around the polymer have an inherent structure for each polymers. What kind of changes would occur in the water structure where protein and polymer exist in the aqueous medium simultaneously? Does the change of the water structure affect the environment around the protein and make any influence on the structure of the protein? We studied the denaturation of proteins and change in the water structure in aqueous medium containing protein and water-soluble polymer by using Raman spectroscopy.

The bovine serum albumin (BSA) was used as protein, and poly(ethylene glycol) (PEG) and poly(2-methacryloyloxy ethyl phosphorylcholine) (PMPC) having phospholipid polar group were used as polymers. The latter two polymers are widely used in the biomedical field. Water molecules in the PMPC aqueous solution and hydrated gel show the bulk water-like structure, which is confirmed by the thermal analysis. Thus a weak interaction was observed between the PMPC and water molecules. A phosphate buffered solution (PBS) involving BSA and polymer was prepared.

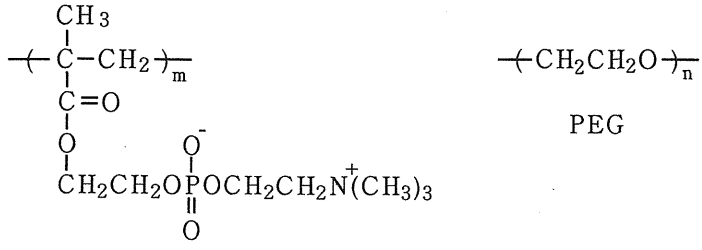

Fig. 28 Structures of Polymers

First we invesigate Raman spectra of the BSA solution excited by a near-infrared laser at 1064 nm are shown in Fig. 28.

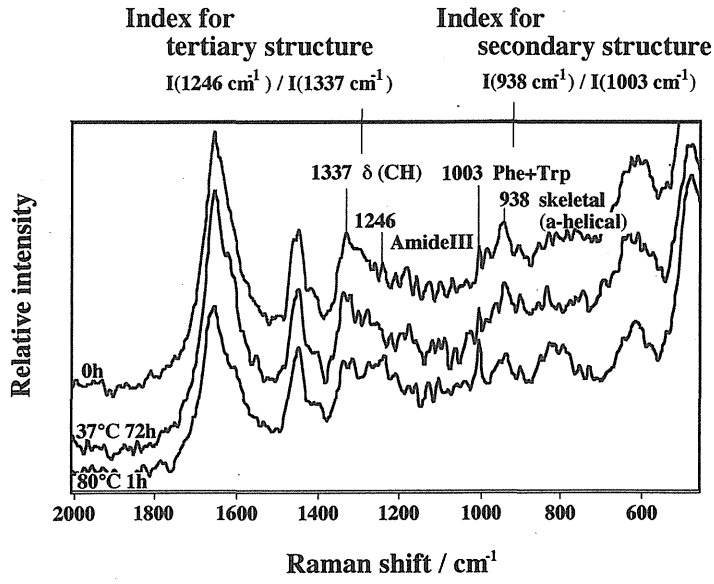

Fig. 29 Raman Spectra of BSA Solution

Measured by Bomem Fourier transform spectrometer, DA8.3, excited by YAG laser fundamental line at 1064 nm. Resulution is set to 10 cm^{-1}, 4 spectra were coadded, each of them was constructed with 4000 scans (which take about 3 hrs) .

The upper curve is the spectrum of fresh BSA, the middle curve is that after incubation for 72 h at 37℃, and the lower curve is that after incubation for 1 h at 80℃. The intensity of the peak at 938 cm^{-1} indicates the content of α-helix in BSA. The intensity at 938 cm^{-1} decreased against an increase of the incubation time. It is reported that the intensity of the peak at 1003 cm^{-1} assignable to phenylalanine and tryptophane residues in BSA keep constant against the denaturation of protein. Therefore, the intensity ratio I(938 cm^{-1})/I(1003 cm^{-1}) indicates the extent of the change in the secondary structure. We will define the ratio of the intensities of the 938 cm^{-1} and 1003 cm^{-1} bands as an index for the secondary structure (ISS) of the protein.

On the other hand, the ratio of the intensities of the 1246 cm^{-1} and 1337 cm^{-1} bands, I(1246 cm^{-1})/I(1337 cm^{-1}), will be used as an index for the tertiary structure (ITS) of the protein. The peak at 1246 cm^{-1} reflects the amide III mode of vibration of the protein and the peak at 1337 cm^{-1} is assignable to the CH group of the protein. The meanings of the index for secondary structure and the index for tertiary structure are shown in Fig. 30.

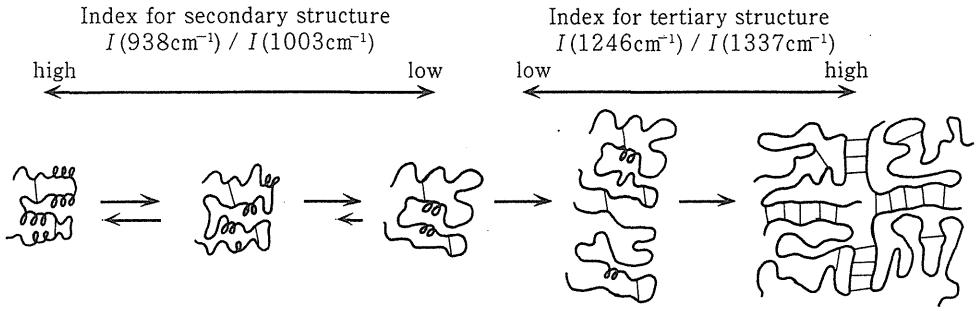

Fig. 30 Meaning of ISS and ITS

When the denaturation of protein starts, the decrease of ISS and increase of ITS were both observed. The relation between the indices and incubation time of BSA solution is shown in Fig. 31.

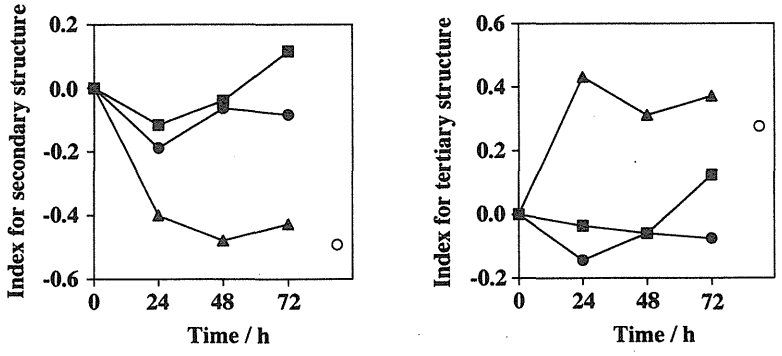

Fig. 31 Relation between Conformational Change of BSA and Incubation Time

● : 5 wt% BSA in PBS,
▲ : 5 wt% BSA + 5 wt% PEG in PBS,
■ : 5 wt% BSA + 5 wt% PMPC in PBS,
○ : 5 wt% BSA in PBS incubated at 80℃ for 1 h.

For ISS, the change of the values was not observed in BSA solution with and without PMPC during 72 h-incubation. Whereas the ISS of BSA solution containing PEG decreased considerably for 24 h, and then became constant afterward. For ITS, on the other hand, the BSA solution with and without PMPC did not show any chnage for 72 h-incubation. But the BSA solution containing PEG showed the increase of ITS for 24 h-incubation and then kept constant value of ITS.

These results suggest that the change of both secondary and tertiary structures of BSA occurs in PEG solution for 24 h-incubation, while BSA in PBS and PMPC solution is not denatured during 72 h-incubation.

Next we investigated Raman spectrum of water excited at 514.5 nm by Ar ion laser (Fig. 32).

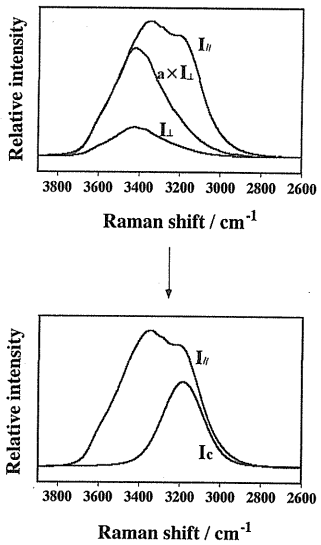

Fig. 32 Raman Spectra of Water

Measured by Dilor laser Raman spectrometer, model XY.

We used the method proposed by Green and co-workers, which is described in section 6-2, to separate the spectral component which reflects the water molecules constructing a microcluster structure. As has been examined in many aqueous systems, the collective motion does not contribute to the intensity of the O-H stretching band at higher frequency side. Next we assume that the depolarization ratio is not frequency dependent but constant in the frequency region in question. Then the equation 21) can be rewritten as follows

$$I_{/\!/}^{am}(\omega) = a\, I_{\perp}^{am}(\omega) \qquad 23)$$

where a is the reciprocal of the depolarization ratio ρ as defined in equation 20) but is now a constant. The determination of a can be carried out graphically on a computer display. That is, the spectral curve of the $I_{\perp}^{am}(\omega)$ component is multiplied by any number such that the resultant curve of the higher frequency side coincide with that of the spectral curve of the $I_{/\!/}^{am}(\omega)$ component (or apparent $I_{/\!/}(\omega)$ curve). The spectral curve thus calculated is a $I_{\perp}^{am}(\omega)$. $I_c(\omega)$ component is calculated as the difference of $I_{/\!/}(\omega)$ and a $I_{\perp}^{am}(\omega)$ as represented by equation 21). The spectrum thus obtained is called as the collective band.

It is believed that the free water molecules construct cluster structures in liquid. Also the water molecules surrounding hydrophobic substance take the same structure as those of the clusters.

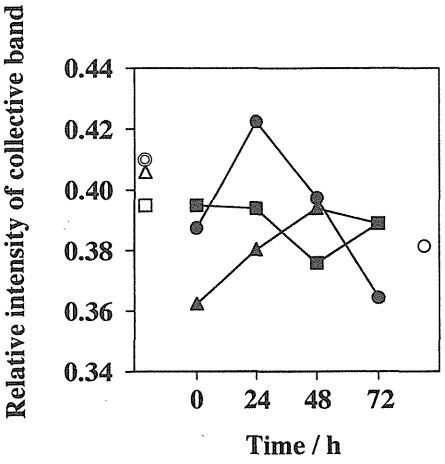

Fig. 33 Relation of the Relative Intensity of Collective Band and Incubation Time

● : 5 wt% BSA in PBS,
▲ : 5 wt% BSA + 5 wt% PEG in PBS,
■ : 5 wt% BSA + 5 wt% PMPC in PBS,
◎ : PBS, △ : 5 wt% PEG in PBS,
□ : 5 wt% PMPC in PBS,
○ : 5 wt% BSA in PBS incubated at 80℃ for 1 h.

The intensity of the collective band of BSA and polymer solutions is shown in Fig. 33. The intensity of the collective band of BSA solution decreased just after the dissolving of BSA in PBS. The intensity kept increasing for 24 h of incubation, but it went decreasing immediately after 24 h. Whereas in PEG solution, the intensity of the collective band decreased just after the dissolving of BSA, and then it kept increasing for 24 to 48 h of incubation. On the other hand, the change of the intensity in PMPC solution was not observed, even when BSA was dissolved.

From these results, we will make a speculation for the effect of water structure in the BSA solution on the structure of BSA. When BSA is dissolved in PBS, water molecules construct the hydrophilic hydration layer around BSA. While a long incubation time, there has not been observed any denaturation of BSA, but the number of water molecules which construct a hydrophilic hydration layer seems to be increasing. Therefore, the intensity of the cluster decreases over 24 h incubation time.

In PEG solution, there exists a water layer where the water molecules construct a hydrophobic hydration around PEG chains. When BSA is dissolved in the solution, the proteins try to make a hydrophilic hydration layer around themselves. Therefore, the water molecules should be shared between PEG and BSA, and there occurs the distortion of cluster-like water structure by the dissolution of BSA. Since the BSA molecules could not construct hydration layer around themselves, they are forced to be danaturated. In this process, the hydrophobic groups in BSA are organized outside the molecule. The water molecules around BSA are reformed to the structure as the same as that around PEG. Consequently, the intensity of the collective band increases.

In PMPC solution, the water molecules construct a bulk water-like structure around PMPC chains. Since the BSA protein molecules can construct a hydration layer around themselves, the protein is not denaturated and the water molecules keep the cluster-like structure.

These results show a close correlation between water, polymers, and proteins with each other. In conclusion, the structure of the water molecules surrounding proteins affects significantly the denaturation of proteins.

…One is reminded of the story of the drunk who, one dark night, has lost his keys. He is seen looking for them under a street light. When asked where he lost them, he points across the street, where all is dark. "Why, then, are you looking for them here?" He replies, "Because there is more light here"……[100].

We hope that a piece of work we are trying to clarify the role of water in biological system is one of the researches directing toward the final goal of understanding of molecular mechanism in life, although the street is still not bright enough.

References

<Book and Reviews>

1) D. Eisenberg and W. Kauzmann, "The Structure and Properties on Water", Oxford (1969); Japanese edition by S. Seki and T. Matsuo, Misuzu-Shobo Tokyo (1975).

2) F. Franks ed. "Water, a comprehensive treatise" vol. 1~7 (1972~1982).

3) K. Suzuki, "Water and Aqueous Solutions" (in Japanese) Kyoritu Shuppan (1980).

4) K. Suzuki, "The Current of Research on Water Structure and Hydrophobic Interaction - On the Extension of Research since Professor Kauzmann" (in Japanese) Hyomen **34**(1), 43-51 (1996).

5) Feature articles on "The Wonders of Water" (in Japanese) Kagaku, **51**(11), 672-698 (1989).
6) K. Tamaru ed. "Material Science I" (in Japanese) Chap. 7～11, The Univ. of the Air, (1987).
<Monomer>
7) G. Herzberg, "Molecular Spectra and Molecular Structure Ⅲ. Electronic Spectra and Electronic Structure of Polyatomic Molecules" D. van Nostrand Company, New York (1966).
8) T. Oka and Y. Morino, J. Mol. Spectrosc., **6**, 472-482 (1961).
9) B.T. Darling and D.M. Dennison, Phys. Rev. **57**, 128-139 (1940).
10) H.H. Nielsen, Rev. Mod. Phys., **23**, 90-136 (1951).
11) R.L. Cook, F.C. Delucia, and P. Helminger, J. Mol. Spectrosc., **53**, 62-76 (1974).
12) W.S. Benedict, N. Gailar, and E.K. Plyler, J. Chem. Phys., **24**, 1139-1165 (1956).
13) "Landolt-Boernstein New Series Vol.7", J.H. Callomon, E. Hirota, K. Kuchitsu, W.J. Lafferty, A.G. Maki, and C.S. Pote, Springer-Verlag Berlin (1976).
14) A. Hoy and P.R. Bunker, J. Mol. Spectrosc., **74**, 1-8 (1979).
15) J.T. Hougen, P.R. Bunker, and J.W.C. Johns, J. Mol. Spectrosc., **34**, 136-172 (1970).
16) P. Jensen and P.R. Bunker, J. Mol. Spectrosc., **118**, 18-39 (1986).
17) P. Jensen, J. Mol. Spectrosc., **133**, 438-460 (1989).
18) R. Bartlett, S.J. Cole, G.D. Purvis, W.C. Hsieh, I. Shavitt, J. Chem. Phys., **87**, 6579-6591 (1987).
19) P. Jensen, J. Mol. Spectrosc., **128**, 478-501 (1988).
20) P. Jensen, S.A. Tashkun, and VL.G. Tyuterev, J. Mol. Spectrosc., **168**, 271-289 (1994).
21) L.H. Coudert, J. Mol. Spectrosc., **165**, 406-425 (1994).
22) S.E. Choi and J.C. Light, J. Chem. Phys., **97**, 7031-7054 (1992).
<Dimer>
23) M. van Theil, E.D. Becker, and G.C. Pimentel, J. Chem. Phys., **27**, 486-490 (1957).
24) A.J. Tursi and E.R. Nixon, J. Chem. Phys., **52**, 1521-1528 (1970).
25) L.L. Shipman, J.C. Owicki, and H.A. Scherage, J. Phys. Chem., **78**, 2055-2060 (1974).
26) H. Kistenmacher, G.C. Lie, H. Popkie, and E. Clementi, J. Chem. Phys., **61**, 546-561 (1974).
27) G.P. Ayers and A.D.E. Pulli, Spectrochim. Acta, **32A**, 1629-1639 (1975).
28) T-L. Tso and E.K.C. Lee, J. Phys. Chem., **89**, 1612-1618 (1985).
29) R.L. Redington and D.E. Milligan, J. Chem. Phys., **39**, 1276-1284 (1963).
30) D. Forney, M.E. Jacox, and W.E. Thompson, J. Mol. Spectrosc., **157**, 479-493 (1993).
31) F.T. Greene and T.A. Milne, J. Chem. Phys., **39**, 3150-3151 (1963).
32) T. R. Dyke and J.S. Muenter, J. Chem. Phys., **57**, 5011-5012 (1972).

33) T. R. Dyke, K.M. Mack, and J.S. Muenter, J. Chem. Phys., **66**, 498-510 (1977).
34) J.A. Odutola and T.R. Dyke, J. Chem. Phys., **72**, 5062-5070 (1980).
35) G.T. Fraser, R.D. Suenram, L.H. Coudert, and R.S. Frye, J. Mol. Spectrosc., **137**, 244-247 (1989).
36) E. Zwart, J.J.Ter Meulen, and W.L. Meerts, Chem. Phys. Lett., **166**, 500-502 (1990).
37) J.T. Hougen, J. Mol. Spectrosc., 114, 395-426 (1985).
38) L.H. Coudert and J.T. Hougen, J. Mol. Spectrosc., **130**, 86-119 (1988).
39) L.H. Coudert and J.T. Hougen, J. Mol. Spectrosc., **139**, 259-277 (1990).
40) G.T. Fraser, Int. Rev. Phys. Chem., **10**, 189-206 (1991).
41) N. Pugliano and R.J. Saykally, J. Chem. Phys., **96**, 1832-1839 (1992).
42) M.F. Vernon, D.J. Krajnovich, H.S. Kwok, J.M. Lisy, Y.R. Shen, and Y.T. Lee, J. Chem. Phys., **77**, 47-57 (1982).

<Trimer>

43) O. Matsuoka, E. Clementi, and M. Yoshimine, J. Chem. Phys., **64**, 1351-1361 (1976).
44) H. Kistenmacher, G.C. Lie, H. Popkie, and E. Clementi, J. Chem. Phys. **61**, 546-561 (1974).
45) R. M. Bentwood, A.J. Barnes, and W.J. Orville-Thomas, J. Mol. Spectrosc., **84**, 391-404 (1980).
46) A. Engdahl and B. nelander, J. Chem. Phys., **86**, 4831-4837 (1987).
47) N. Puglians and R.J. Saykally, Science, **257**, 1937-1940 (1992).
48) R.J. Saykally and G.A. Blake, Science, **259**, 1570-1515 (1993).
49) K. Liu, M.J. Elrod, J.G. Loeser, J.D. Cruzan, N. Pugliano, M.G. Brown, J. Rzepiela, and R.J. Saykally, Faraday Discuss., **97**, 35-41 (1994).
50) O. Mo, M. Yanez, and J.Elyuero, J. Chem. Phys., **97**, 6628-6638 (1992).
51) M. Schuetz, T. Buergi, S. Leutwyler, and H.B. Buergi, J. Chem. Phys., **99**, 5228-5238 (1993).
52) S.S. Xantheas and T.H. Dunning Jr., J. Chem. Phys., **99**, 8774-8792 (1993).
53) D.J. Wales, J. Am. Chem. Soc., **115**, 11180-11190, 11191-11201 (1993).
54) J.G.C.M. van Duijneveldt-van de Rijdt and F.B. van Duijneveldt, Chem. Phys., **175**, 271-281 (1993).

<Ice>

55) S.W. Peterson and H.A. Levy, Acta Cryst., **10**, 70-76 (1957).
56) E. Whally and J.B.R. Heath, J. Chem. Phys., **45**, 3976-3982 (1966).
57) W.F. Giauque and J.W. Stout, J. Am. Chem. Soc., **58**, 1144-1150 (1936).
58) L. Pauling, "The Nature of the Chemical Bond", 3rd ed., Cornell Univ. Press, Ithaca, New York (1960).

<Liquid>

59) J. Morgan and B.E. Warren, J. Chem. Phys., **6**, 666-673 (1938).
60) A.H. Narten, M.D. Danford, and H.A. Levy, Disc. Faraday Soc., **43**, 97-107 (1967).
61) G. Nemethy and H.A. Scheraga, J. Chem. Phys., **36**, 3382-3400, 3401-3417 (1962).

62) Ya.O. Samoilov, "Структука Водных Растворов Электролитови Тиоратация Ионов", Издательство Академии Наук СССР, Москва (1957); Japanese translation by Wataru Uehira "Hydration of ion", Chijin Shoten (1967).
63) J.A. Pople, Proc. Roy. Soc., **A205**, 163-178 (1951).
64) S.A. Rice and M.G. Sceats, J. Phys. Chem., **85**, 1108-1119 (1981).
<Molecular dynamics>
65) A. Rahman and F.H. Stillinger, J. Chem. Phys., **55**, 3336-3359 (1971).
66) F.H. Stillinger and T.A. Weber, Phys. Rev., **25**, 978-989 (1982).
67) F.H. Stillinger and T.A. Weber, Phys. Rev., **28**, 2408-2416 (1983).
68) F.H. Stillinger and T.A. Weber, J. Phys. Chem., **87**, 2833-2840 (1983).
69) H. Tanaka and I. Ohmine, J. Chem. Phys., **87**, 6128-6139 (1987).
70) I. Ohmine, H. Tanaka, and P.G. Wolynes, J. Chem. Phys., **89**, 5852-5860 (1988).
71) M. Sasai, I. Ohmine, and R. Ramaswamy, J. Chem. Phys., **96**, 3045-3053 (1992).
<IR of monomer>
72) L.A. Pugh and K. Narahari Rao, J. Mol. Spectrosc., **47**, 403-408 (1973).
73) C. Camy-Peyret, J.-M. Flaud, J.-P. Maillard, and G. Guelachvili, Mol. Phys., **33**, 1641-1650 (1977).
74) L.H. Coudert, J. Mol. Spectrosc., **165**, 406-425 (1994).
75) R.J. Bartlett, S.J. Cole, G.D. Purvis, W.C. Ermler, H.C. Hsieh, and I. Shavitt, J. Chem. Phys., **87**, 6579-6591 (1987).
76) S.E. Choi and J.C. Light, J. Chem. Phys., **97**, 7031-7054 (1992).
77) N.J. Bramley and T. Carrington, Jr., J. Chem. Phys., **99**, 8519-8541 (1993).
<Raman spectrum of liquid>
78) J.R. Scherer, M.K. Go, and S. Kint, J. Phys. Chem., **78**, 1304-1312 (1974).
79) P.T.T. Wong and E. Whalley, J. Chem. Phys., **62**, 2418-2425 (1975).
80) G. Nielson and S.A. Rice, J. Chem. Phys., **78**, 4824-4827 (1983).
81) T.C. Sivakumar, S.A. Rice, and M.G. Sceats, J. Chem. Phys., **69**, 3468-3476 (1978).
82) M.S. Bergren, D. Schuh, M.G. Sceats, and S.A. Rice, J. Chem. Phys., **69**, 3477-3482 (1978).
83) R. McGraw, W.G. Madden, M.S. Bergren, S.A. Rice, and M.G. Sceats, J. Chem. Phys., **69**, 3483-3496 (1978).
84) W.G. Madden, M.S. Bergren, R. McGraw, S.A. Rice, and M.G. Sceats, J. Chem. Phys., **69**, 3497-3501 (1978).
85) M.S. Bergren and S.A. Rice, J. Chem. Phys., **77**, 583-602 (1982).
86) E. Walley, Can. J. Chem., **55**, 3429-3441 (1977).
87) J.L.Green, A.R. Lacey, and M.G. Sceats, J. Phys. Chem., **90**, 3958-3964 (1986).
88) J.L.Green, A.R. Lacey, and M.G. Sceats, J. Chem. Phys., **86**, 1841-1847 (1986).
89) J.L.Green, A.R. Lacey, M.G. Sceats, S.J. Henderson, and R.J. Speedy, J. Phys. Chem., **91**, 1684-1686 (1987).
90) J.L.Green, A.R. Lacey, and M.G. Sceats, Chem. Phys. Lett., **134**, 385-391 (1987).

91) J.L.Green, A.R. Lacey, and M.G. Sceats, Chem. Phys. Lett., **137**, 537-542 (1987).
92) J.L.Green, A.R. Lacey, and M.G. Sceats, J. Chem. Phys., **87**, 3603-3610 (1987).
93) T. Terada, Y. Maeda, and H. Kitano, J. Phys. Chem., **97**, 3619-3622 (1993).
94) Y. Maeda, N. Tsukida, H. Kitano, T. Terada, and J. Yamanaka, J. Phys. Chem., **97**, 13903-13906 (1993).
95) G.E. Walrafen, in F. Frank (ed.), "Water -a Comprehensive Treatise", Vol.1 Chap. 5, Plenum Press, New York (1971).
96) Y. Maeda and H. Kitano, Spectrochim. Acta, **A51**, 2433-2446 (1995).
<Hydration of polymer>
97) R. Cooke and I.D. Kuntz, Ann. Rev. Biophys. Bioeng., **3**, 95-126 (1974).
98) H. Uedaira, Hyomen, **13**, 297-307 (1975).
99) J.A. Ernst, R.T. Clubb, H-X. Zhou, A.M. Gronenborn, and G.M. Clore, Science, **267**, 1813-1817 (1995).
100) W. Kauzmann, Nature, **325**, 763-764 (1987).

(平成8年11月18日受理)